Published in final edited form as:
Biomacromolecules. 2011 December 12; 12(12): 4319–4325. doi:10.1021/bm201246f.

Robust and Responsive Silk Ionomer Microcapsules

Chunhong Ye[a,b], **Olga Shchepelina**[b], **Rossella Calabrese**[c], **Irina Drachuk**[b], **David L. Kaplan**[c], and **Vladimir V. Tsukruk**[b,*]

[a]School of Chemical Engineering, Nanjing Forestry University, Nanjing, Jiangsu 210037, P. R. China

[b]School of Materials Science and Engineering, Georgia Institute of Technology, Atlanta, Georgia 30332 (USA)

[c]Department of Biomedical Engineering, Tufts University, 4, Colby street, Medford, MA 02155 (USA)

Abstract

We demonstrate the assembly of extremely robust and pH-responsive thin shell LbL microcapsules from silk fibroin counterparts modified with poly(lysine) and poly(glutamic) acid which are based on biocompatible silk ionomer materials in contrast to usually exploited synthetic polyelectrolytes. The microcapsules are extremely stable in the unusually wide pH range from 1.5 to 12.0 and show remarkable degree of reversible swelling/deswelling response in dimensions as exposed to extreme acidic and basic conditions. These changes are accompanied by reversible changes in shell permeability which can be utilized for pH-controlled loading and unloading of large macromolecules. Finally, we confirmed that these shells can be utilized to encapsulate yeast cells with viability rate much higher than that for traditional synthetic polyelectrolytes.

INTRODUCTION

Thin shell microcapsules with responsive properties and controlled permeability have potential applications in the field of drug delivery, biosensing, food industry, biology and biomedicine.[1,2,3,4,5,6] The most useful microcapsules for bio-related applications should be biocompatible, non-cytotoxic, mechanically robust and elastic microcapsules which are stable in a wide range of environmental conditions, have high encapsulation efficiency, controlled or switchable permeability, and can be easily prepared.[7] Several approaches have been suggested to fabricate various soft microcapsules, such as interfacial emulsion polymerization,[8] layer-by-layer (LbL) assembly of polymers by H-bonding or covalent bands,[9] and self-assembly of block copolymers.[2] However, there are a number of common problems associated with these fabrication approaches including high polydispersity, uneven shell coverage, aggregation and system solidification. Lipid-based liposomes are another approach, but limited stability and low permeability for polar molecules present limitations for general use.[10]

A simple and high yield route using LbL adsorption of oppositely charged polyelectrolytes in decomposable particles, followed by core removal,[11] has been widely used for microcapsule fabrication.[12,13,14] To date a series synthetic polymers, biological components, and nanoparticles have been employed to obtain microcapsules.[15,16,17,18,19,20,21,22] For drug delivery system, the potential use of microcapsules requires the capability of releasing active compounds in certain pH, because some regions of body appear to have lower pH than

*Corresponding author. Vladimir@mse.gatech.edu.

normal ones due to pathological conditions such as inflammation, infection or malignancy;[23] Furthermore, the microcapsule should be stable for protecting entrapped molecules from degradation or denaturization, biocompatible and biodegradable which is critical for biosensing applications.[24] The major limitations of this approach are cytotoxicity of cationic components and poor stability of microcapsules at extreme acidic and basic condition with capsules heavily irreversibly deformed or dissolved completely.[25,26] Thereby, the choice of proper components for biocompatible microcapsules is limited, and stable and reversibly deformable microcapsules at extreme acidic and basic conditions are rare.

Natural protein, such as silk fibroin, might be considered for construction of such microcapsules. Silk as a natural protein from silkworms and spiders has been widely employed for a variety of biomedical and biotechnological applications.[27,28] The attraction of silk fibroin is due to its biocompatible, biodegradable, versatile materials fabrication options and extraordinary mechanical properties.[29,30,31] Under certain conditions of pH, temperature or ionic strength, silk proteins form supermolecular structures in the form of hydrogels, films, sponges, fibers and ropes which depend on the processing method.[32] Silk-based materials also stabilize the activity of enzymes and biomolecules in harsh environment.[33] Silk capsules have been reported to be formed by interfacial adsorption method,[34] which was fast and produced robust microcapsules, but required the transfer of the capsules from the emulsion into a single-phase solution. Overall, building microcapsules from proteins is challenging, because protein assemblies are not very stable in this format. Indeed, our recent study showed successful fabrication of silk microcapsules via LbL assembly based upon hydrophobic-hydrophobic interactions, although they remained modestly robust and stable only within a narrow pH interval.[35]

Herein, we demonstrate robust silk microcapsules which are stable at extreme pH conditions, undergo reversible swelling/deswelling behavior and tunable permeability, all facilitated by additional ionic interactions and cross linking of silk-based copolymers. These silk ionomer capsules demonstrated pH triggered responses at extreme acidic (pH<2.5) and basic (pH>11) conditions with many fold volume increases without compromising capsule disintegration. Such pH-induced changes in capsule size and shell permeability were utilized to demonstrate the encapsulation and release of large macromolecules by changing environmental conditions. Moreover, these shells can be utilized to directly encapsulate yeast cells with viability rate much higher than that for traditional synthetic polyelectrolytes.

EXPERIMENTAL

Materials

Poly(amino acid) modified silk materials were obtained using our previously published methods that involve diazonium activation of the abundant tyrosine side chains in the silk fibroin chains, followed by chemical linking with polylysine or polyglutamic acid (Fig. 1).[32] The silk fibroin was extracted from *Bombyx mori* cocoons according to established procedure[36]. Firstly silk fibroin was enriched in carboxyl content, then one of the silk-poly(amino acid)-based ionomer (SF-PG) was obtained by grafting poly-glutamic acid on silk fibroin (SF) to achieve a high content of carboxyl group. On the other hand, SF-PL represents the silk fibroin modified with polylysine to enrich the amine group content.

Silica spheres with a diameter of 4.0±0.2 μm were obtained from Polysciences, Inc as water 10% dispersions. Sodium phosphate dibasic, sodium phosphate monobasic, Hydrofluoric acid (48–51%) were obtained from BDH company. Polyethylenimine (PEI) with M_n = 10,000 was obtained from Sigma-Aldrich. The cross-linker, 1-ethyl-3-[3-dimethylaminopropyl] carbodiimide hydrochloride (EDC), was obtained from TCI. Fluorescent isothiocyanate (FITC) and FITC-Dextrans with different molecular weights

were purchased from Sigma-Aldrich. The S. *cerevisiae* YPH501 diploid yeast cells were used for cell encapsulation in accordance with usual procedure published elsewhere.[37] Briefly, cells were cultured in synthetic minimal medium (SMM) supplemented with necessary nutrients and sugar source, 2% glucose. Cells were harvested at early log phase with optical density (OD) ~0.3–0.4. Glucose was purchased from Sigma-Aldrich. Live-dead cell staining kit was purchased from Biovision. All the solutions were filter-sterilized with polystyrene nonpyrogenic membrane systems (0.22 μm pore size) (Corning filter system) before applying to the cells. All the water used in this study was Nanopure water with resistivity above 18.2 MΩ cm.

Fabrication of "PEI-(SF-PG/SF-PL)" Capsules

Silica spheres were dispersed in 0.5mg/ml PEI solution (prepared in 0.1M NaCl, pH 7) to make a prime layer to stabilize LbL process. Then silica spheres were dispersed in 1mg/ml silk fibroin-poly glutamic acid, SF-PG, prepared in 0.05M phosphate buffer at pH 5.5, followed by three times cycle wash by redispersion in phosphate buffer at pH 5.5 and centrifugation at 1,000 rpm for 1 min to remove the excess polyelectrolyte. The SF-PL deposition was carried out by redispersion in 1mg/ml silk fibroin-poly lysine solution, prepared in 0.05M phosphate buffer at pH5.5 followed by the same washing procedure described above.

Multilayer capsules were obtained by repeating the alternating deposition of SF-PG and SF-PL components (Fig. 2). Each deposition was carried out at slow rotation avoiding formation of air bubbles for 15 min, followed by 3 wash cycles. All capsules presented in this study were cross-linked by introduced 1-ethyl-3-[3-dimethylaminopropyl] carbodiimide hydrochloride (EDC) according the established procedure.[26] Silica spheres with alternating SF-PG/SF-PL multilayers were added to 5 mg/ml EDC solution (prepared in 0.05M phosphate buffer at pH 5.5) for 40min, then washed with phosphate buffer at pH 5.5 to remove the excess coupling agent. To dissolve silica cores, the particles were exposed to HF/ NH_4F solution (pH≈5.5) overnight, followed by dialysis against Nanopure water at pH 5.5 for 72 hours (Fig. 2).[32,38,39]

Zeta-Potential Measurements

Surface potentials of silica sphere after every deposited layer and hollow capsules at wide pH range from 1.5 to 12 were measured on Zetasizer Nano-ZS (Malvern). Each value was obtained by averaging three independent measurements of 30 runs each.

Atomic Force Microscopy (AFM)

Surface topography of the hollow capsules in dry state was examined on AFM.[40] The height and phase images were collected from Dimension-3000 (Digital Instruments) in tapping mode using silicon V-shape cantilevers having spring constant of 46 N/m. The capsule single wall thickness was determined as half of the height of the collapsed flat regions on dried capsules using bearing analysis from NanoScope software to generate height histograms.[41,42]

Scanning Electron Microscopy (SEM)

SEM analysis was performed on Hitachi S-3400-IIscanning electron microscope at 10 kV. Before imaging, capsules were air-dried on pre-cleaned silicon wafer and sputter-coated with gold layer.

Confocal Laser Scanning Microscopy (CLSM)

Confocal images of capsules were obtained with LSM 510 Vis confocal microscopy equipped with 63×1.4 oil immersion objective lens (Zeiss). Capsules were visualized by adding FITC solution (1mg/ml in phosphate buffer at pH 5.5) to capsule suspension in Lab-Tek chambers (Electron Microscopy Science). Excitation/emission wavelengths were 488/515nm. To investigate capsule pH responsive property, a drop of capsule suspension was added to several Lab-Tek chambers, mixed with a drop of FITC solution (1 mg/ml in phosphate buffer at pH 5.5). Then the chamber was 3/4 filled with 0.05M phosphate buffer at different pH. To investigate the pH reversible responsive property, a drop of capsule mixed with FITC at pH 5.5 was added to a Lab-Tek chamber, and the chamber was 3/4 filled with phosphate buffer at pH 11.5. After CLSM images were taken, the liquid in the chamber was sucked out. The chamber was refilled with another phosphate buffer at pH 7.5. Then this alternative pH treatment cycle was repeated several times. To check capsule permeability to FITC-Dextrans, a drop of capsule was added to several Lab-Tek chambers, which were then filled with 1 mg/ml FITC-Dextran solution (prepared in phosphate buffer at pH 5.5).

Encapsulation of cells with silk ionomer shells

Yeast cells were grown at 30°C in a shaker incubator (New Brunswick Scientific) with 225 rpm to bring them to an early exponential phase [with optical density at 600nm (OD600 test) =0.3–0.4].[37] For comparison, we encapsulated yeast cell by the same procedure as PEI-(SF-PG/SP-PL) microcapsules mentioned above. Before deposition of the PEI-(SF-PG/SF-PL) shell, yeast cells were harvested in 1.5 ml microcentrifuge tubes at 2000rpm for 2min and washed three times in phosphate buffer (0.01M in 0.1M NaCl, pH=6). First, a precursor, PEI (0.5 mg/ml in 0.1M NaCl, pH=7), was employed, followed by consecutive deposition of SF-PG and SF-PL. After deposition of each layer, cells were washed three times by phosphate buffer. Three bilayers were employed in this study, followed by cross linking with EDC for 20 minutes. The viability of yeast cells was assessed by using a live-dead cell staining kit. Images were collected with LSM 510 Vis confocal microscopy equipped with 63×1.4 oil immersion objective lens. The viability was estimated by counting the number of viable and dead cells in images acquired in different sections.

RESULTS AND DISCUSSION

Silk-based copolymers utilized here contain oppositely charged lysine (SF-PL) and glutamate acid (SF-PG) alternating layers to facilitate ionic pairing to enhance LbL construction of stable ultrathin shells (Fig. 1). These polyelectrolytes have been obtained by selective modification of functional side groups of the silk protein polymer backbone to add either cationic or anionic amino acid pendant groups as described elsewhere.[32] As has been demonstrated, these silk ionomers are sensitive to controlled complexation in solution and undergoing complexation behavior when exposed to the changing pH thus providing a means for responsive behavior.[26,32,43,44]

In this study, LbL assembly was carried out at mild pH (pH 5.5, 0.05M phosphate buffer solution) to minimize structural changes of the capsule and maximize ionic interactions for enhanced stability. Furthermore, all the capsules were employed with a PEI prelayer to ensure effective LbL assembly. In addition, covalent cross-linking was introduced between pendant groups of SF-PL and SF-PG using 1-ethyl-3-[3-dimethylaminopropyl] carbodiimide hydrochloride as a cross-linking agent to provide stable shape of capsule while silk ionomers lost negative/positive charge at extreme acid (pH 1–2) and basic (pH 11–12) (Fig. 2).[26]

In order to gain a better understanding of the stepwise growth of the multilayer shells on silica spheres at pH 5.5, ζ-potential was monitored for the particles after each deposition

step (Fig. 3-a). At pH 5.5, SF-PG is negatively charged (p*Ka* of poly-glutamic acid is around 3.5), while SF-PL is positively charged (p*Ka* of polylysine is around 9).[45] The original silica spheres have a ζ-potential of around -35 mV. The ζ-potential alternates after each SF-PG and SF-PL layer deposition, which indicates a common charge-overcompensated mechanism of LbL shell formation and step-wise growth of silk shells around the silica particles.

The thickness of silk ionomer capsule shells with different bilayers was measured by AFM cross-sections in dry state (Fig. 3-b and Fig. 4). The AFM images of capsules composed of 3, 5, 7, 9 bilayers, after being placed on a silicon wafer, have been collapsed upon drying with many random wrinkling due to capillary forces. This observation was confirmed by SEM images of coated particles and silk shells after core release (Fig. 5-a and Fig. 5-b).[46,47,48]

The shell thickness increased from 19±1 nm to 277±11 nm with an increasing number of bilayers (Fig. 3-b). Unlike the silk-on-silk shells based upon hydrophobic interactions with a linear growth mode with an average increment of 4 nm per bilayer, the LbL assembly of silk ionomers exhibited an exponential growth which is common for many biopolyelectrolytes including poly-lysine/poly glutamic acid LbL films with intense interfacial diffusion processes and efficient complexation.[49,50,51]. The microroughness of shells also increased from 4.4 nm to 11.4 nm (as measured in selected areas of 1×1 μm), a common phenomenon for diffusion-enhanced LbL assembly with aggregated and porous morphologies.[52]

The drying hollow capsules collapsed due to capillary forces with random folding patterns common for uniform shells (Fig. 5).[53,54] High-resolution AFM images revealed a grainy texture which is associated with the microphase morphology of silk materials undergoing partial transformation of secondary structure during drying.[55] Confocal images of capsules shells labeled by fluorescent isothiocyanate (FITC) shows the hollow structure of capsule after the silica core is dissolved (Fig. 5-d). All capsules possess very uniform shapes and diameters around 3.6 μm which is close to the original core diameter considering some shell contraction.[56]

Next, the silk ionomer capsules were subjected to variations pH to test their stability and responsive behavior. First, the variation of ζ-potential of capsules in a wide pH range from 1.5 to 12.0 was studied (Fig. 6-a). The ζ-potential is a negative constant in the wide pH range from 3.0 to 7.5 and increases to positive values for pH below 2.5 due to the protonation of carboxyl-terminal group on SF-PG below its p*Ka*.[45] On the other hand, capsule potential becomes excessively negative due to the deprotonation of amino groups on the SF-PL above pH 9. Correspondingly, the volume of capsules dramatically increases at these terminal conditions (Fig. 6-b). Capsule diameter with nine bilayers increases from 3.8±0.2 μm to 5.3±0.2 μm (pH 1.5) and 5.7±0.2 μm (pH 12) within ten seconds after changing pH.

On the other hand, the capsule remain stable with unchanged dimensions in a wide range of pH from 2.5 to 11.0 in striking contrast to synthetic LbL shells with significant changes in the vicinity of neutral pH.[57,58] However, in contrast to conventional capsules which are readily dissolved at extreme pHs, crosslinked silk ionomer capsules with the number of bilayers above 7 are capable of multiple and fully reversible shape changes without any residual deformation (Fig. 7). It is worth noting that only capsules with additional covalent cross-linked shells demonstrated extreme stability at basic condition and kept good shape during the reversible pH responsive, although the capsules without cross-linking totally dissolved as exposed to basic (pH>11.5) for 15–20 minutes.

The porous morphology of the silk ionomer shells facilitates their high permeability which, in turn, can be controlled by external pH.[59] To test this ability we exploited the permeability of green-fluorescent FITC-dextrans of various molecular weights at pH 5.5 (Table 1).[34,60,61,62] The thinnest shells (3-bilayers) were permeable to all of the dextrans including 2,000kDa molecular weight, indicating an extremely porous morphology. Increasing the shell thickness resulted in a gradual decrease of cut-off molecular weight down to 4kDa for a 9 bilayer shell, a common trend for LbL capsules which indicates gradual densification of shells and porosity reduction with increasing shell thickness.

The reported hydrodynamic diameters of FITC-Dextran with different molecular weights of 4 kDa, 70 kDa, 150 kDa and 2,000 kDa are 3.30 nm, 11.60 nm, 17.70 nm and 31.8 nm, respectively.[63] Thus we can estimate that the smallest mesh size of the polymer network for the thickest shells is around 7 nm and the largest mesh size of the capsules with a 3-bilayer exceeds 32 nm. The mesh size is easily controlled by the number of silk ionomer bilayers assembled.

Moreover, the loading/unloading behavior of these capsules can be controlled by external pH as was demonstrated by using FITC-dextran as a fluorescent probe (Fig. 8). For instance, 20 kDa dextran did not permeate the shells of 9 bilayer capsules at pH 5.5 (Fig. 8-a), but when the capsules were exposed to the dextran with the same molecular weight at pH 11.5, the “closed” morphology immediately became “open” and highly permeable (Fig. 8-b). Using this approach, FTIC-dextran can be encapsulated by changing the pH of the solution from 11.5 to 7.5 (Fig. 8-c). The encapsulation is very stable, lasting for at least two days. As this capsule solution was adjusted from pH 7.5 to 11.5 again, the encapsulated dextran can be completely released from capsules in 2 hours (Fig. 8-d).

Finally, we conducted preliminary testing of cytotoxicity of silk ionomer shells by encapsulating yeast cells. As known, high cytotoxicity of synthetic LbL shells is caused by the direct contact of cationic polyelectrolytes with cells, which impose formation of pores in the cell membrane followed by severe cell damage and death and thus removal or screening the cationic component has been implemented.[64,65,66] In the case of natural polyelectrolytes, such as silk ionomers studied here, yeast cells encapsulated with PEI-$(SF\text{-}PG/SF\text{-}PL)_3$ shells maintain viability up to 29% in the case of having PEI prelayer and being crosslinked with EDC for 20 min. For cells encapsulated without PEI prelayer and crosslinking agent, viability reached 38%, which is more than twice higher than the 17% viability of cells encapsulated with conventional poly(styrene sulfonate)/poly(allylamine hydrochloride) $(PAH/PSS)_3$ shells as observed in our previous study.[66] Moreover, previous cytocompatibility study of SF-PG and SP-PL by in situ gelation encapsulation human cervical fibroblasts demonstrated exceptionally high cell viability reaching 90%.[32] Cell encapsulation study using LbL assembly of natural polyelectrolytes with improved viability will be discussed elsewhere.

CONCLUSIONS

In conclusion, extremely robust and stable silk ionomer microcapsules were successfully fabricated by combining ionic pairing and covalent crosslinking of functionalized pendant groups. The capsules were stable even at extreme acidic (pH 1–2) and basic (pH 11–12) conditions. The capsules showed significant and highly reversible pH responsive behavior at pH below 2.0 and above 11.0, the maximum volume swelling reaching 800%. Furthermore, these silk ionomer capsules exhibited pH-trigged permeability, thus facilitating pH-controlled encapsulation and release. In comparing to the previous pH trigged capsules composed of synthesis polyelectrolytes by H-bonding or electrostatic interactions, which possess swelling/deswelling behavior usually at mild pH and are deformed or totally

dissolved at strong acid/basic conditions,[20,26] The silk-ionomers capsules with ability to pH-induced encapsulation are important for manipulated loading-unloading of therapeutic cargo and design of biosensing systems.[67] Thereby, the silk ionomer capsules present a promising platform for stable and tunable microcontainers for encapsulation and delivery of small and large macromolecules, nanoparticles, cells, and other species.

Acknowledgments

This work was supported by the Air Force Office of Scientific Research FA9550-08-1-0446, FA9550-09-1-0162, FA9550-10-1-0172 and FA9550-11-1-0233 grants, U.S. Department of Energy, Office of Basic Energy Sciences Award # DE-FG02-09ER46604 and China Scholarship Council 2010832447. The authors thank Dr. Svetlana Harbaugh (Wright Patterson AirForce Base) for providing yeast cell, Dr. Milana Lisunova, Dhaval D. Kulkarni, Zachary Combs and Ikjun Choi (Georgia Institute of Technology) for assistance.

REFERENCES

(1). Caruso F, Caruso RA, Möhwald H. Science. 1998; 282:1111–1114. [PubMed: 9804547]

(2). Discher BM, Won YY, Ege DS, Lee JCM, Bates FS, Dishcher DE, Hammer DA. Science. 1999; 284:1143–1146. [PubMed: 10325219]

(3). Dinsmore AD, Hsu MF, Nikolaides MG, Marques M, Bausch AR, Weitz DA. Science. 2002; 298:1006–1009. [PubMed: 12411700]

(4). Esser-Kahn AP, Odom SA, Sottos NR, White SR, Moore JS. Macromolecules. 2011; 44:5539–5553.

(5). Bédard MF, Geest BG, Skirtach AG, Möhwald H, Sukhorukov GB. Addv. Colloid Interface Sci. 2010; 158:2–14.

(6). Stuart MA, Huck WT, Genezer J, Müller M, Ober C, Stamm M, Sukhorukov GB, Szleifer L, Tsukruk VV, Urban M, Winnik F, Zauscher S, Luzinov L, Minko S. Nature Materials. 2010; 9:101–113.

(7). Gordon VD, Xi C, Hutchinson JW, Bausch AR, Marquez M, Weitz D. A. J. Am. Chem. Soc. 2004; 126:14117–14122.

(8). Jang J, Ha H. Langmuir. 2002; 18:5613–5618.

(9). Huang HY, Remsen EE, Kowalewski T, Wooley KL. J. Am. Chem. Soc. 1999; 121:3805–3806.

(10). Lasic, DD. Liposomes: From Physics to Application. Elsevier; Amsterdam: 1993.

(11). Donath E, Sukhorukov GB, Caruso F, Davis SA, Möhwald H. Angew. Chem. Int. Ed. 1998; 37:2002–2005.

(12). Skirtach AG, Karageorgiev P, Bédard MF, Sukhorukov GB, Möhwald H. J. Am.Chem. Soc. 2008; 130:11572–11573. [PubMed: 18683926]

(13). De Cock LJ, Koker S, Geest BG, Grooten J, Vervaet C, Remon JP, Sukhorukov GB, Antipina MN. Angew. Chem. Int. Ed. 2010; 49:6954–6973.

(14). Decher, G.; Schlenoff, JB.; Lehn, J-M. Multilayer thin films: Sequential Assembly of Nanocomposite Materials. Wiley-VCH; Weinheim, Germany: 2003. p. 1-524.

(15). Wong MS, Cha JN, Choi KS, Deming TJ, Stucky GD. Nano. Lett. 2002; 2:583–587.

(16). Kukula H, Schlaad H, Antomietii M, Forster S. J. Am. Chem. Soc. 2002; 124:1658–1663. [PubMed: 11853440]

(17). Lee D, Rubber MF, Cohen V. Chem. Mater. 2005; 17:1099–1105.

(18). Kim BS, Vinogradova OI. J. Phys. Chem. B. 2004; 108:8161–8165.

(19). Sukhorukov GB, Fery A, Möhwald V. Prog. Polym. Sci. 2005; 30:885–897.

(20). Elsner N, Kozlovskaya V, Sukhishvili SA, Fery A. Soft Matter. 2006; 2:966–972.

(21). Such GK, Tjipto E, Postma A, Johnston APR, Caruso F. Nano Lett. 2007; 7:1706–1710. [PubMed: 17530811]

(22). Ochs CJ, Such GK, Yan Y, Koeverden MP, Caruso F. ACS Nano. 2010; 4:1653–1663. [PubMed: 20201548]

(23). Leroux J, Roux E, Garrec DL, Hong K, Drummond DC. J. Controlled Release. 2001; 72:71–84.

(24). Faraji V, Wipf P. Bioorganic & Medicinal Chemistry. 2009; 17:2950–2962. [PubMed: 19299149]
(25). Déjugnat C, Sukhorukov GB. Langmuir. 2004; 20:7265–7269. [PubMed: 15301514]
(26). Kozlovskaya V, Kharlampieva E, Mansfield ML, Sukhishvili V. Chem. Mater. 2006; 18:328–336.
(27). Hofmann S, Foo CT, Rossetti F, Textor M, Vunjak-Novakovis G, Kaplan DL. J. Controlled Release. 2006; 111:219–227.
(28). Omenetto FG, Kaplan DL. Nat. Photonics. 2008; 2:641–643.
(29). Wang Y, Kim HJ, Vunjak-Novakovis G, Kaplan DL. Biomaterials. 2006; 36:6064–6082. [PubMed: 16890988]
(30). Omenetto FG, Kaplan DL. Science. 2010; 329:528–531. [PubMed: 20671180]
(31). Jin HJ, Kaplan DL. Nature. 2003; 424:1056–1061.
(32). Serban MA, Kaplan DL. Biomacromolecules. 2010; 11:3406–3412. [PubMed: 21028849]
(33). Yu A, Wang Y, Barlow E, Caruso F. Adv. Mater. 2005; 17:1737–1741.
(34). Hermanson KD, Harasim MB, Scheibel T, Bausch AR. Phys. Chem. Chem. Phys. 2007; 9:6442–6446. [PubMed: 18060175]
(35). Shchepelina O, Drachuk I, Gupta MK, Lin J, Tsukruk VV. Adv. Mater. DOI:adma.201102234.
(36). Murphy AR, St John P, Kaplan DL. Biomaterials. 2008; 29:2829–2839. [PubMed: 18417206]
(37). Kozlovskaya V, Harbaugh S, Drachuk V, Shchepelina V, Kelley-Loughnane N, Stone M, Tsukruk VV. Soft Matter. 2011; 7:2364–2372.
(38). Wang YJ, Caruso F. Chem. Commun. 2004; 40:1528–1529.
(39). Shimizu K, Cha J, Stucky GD, Morse DE. Proc. Natl. Acad. Sci. USA. 1998; 95:6234–6238. [PubMed: 9600948]
(40). Tsukruk VV, Reneke DH. Polymer. 1995; 36:1791–1808.
(41). Elsner N, Dubreui F, Fery A. Physical Review E. 2004; 69:031802/1–031802/6.
(42). Mcconney ME, Singamaneni S, Tsukruk VV. Polymer Reviews. 2010; 50:235–286.
(43). Shiratori SS, Rubner MF. Macromolecules. 2003; 33:4213–4219.
(44). Mendelsohn JD, Barrett CJ, Chan VV, Pal AJ, Mayes AM, Rubner MF. Langmuir. 2000; 16:501–5023.
(45). Yu A, Gentle V, Lu V. J. Colloid Interface Sci. 2009; 333:341–345. [PubMed: 19223040]
(46). Wang Y, Caruso F. Chem. Mater. 2005; 17:953–961.
(47). Caruso F. Chem. Eur. J. 2000; 6:413–419. [PubMed: 10747405]
(48). Boulmedais V, Frisch B, Etienne O, Lavalle V, Picart C, Ogier V, Voegel JC, Schaaf P, Egles C. Biomaterials. 2004; 25:2003–2011. [PubMed: 14741614]
(49). Laugel N, Betscha C, Winterhalter M, Voegel V, Schaaf P, Ball V. J. Phys. Chem. B. 2006; 110:19443–19449. [PubMed: 17004803]
(50). Porcel C, Lavalle Ph. Ball V, Decher G, Senger B, Voegel V, Schaaf P. Langmuir. 2006; 22:4376–4383. [PubMed: 16618190]
(51). Lavalle, Ph.; Picart, V.; Mutterer, V.; Gergely, V.; Reiss, H.; Voegel, JC.; Senger, B.; Schaaf, P. J. Phys. Chem. B. 2004; 108:635–648.
(52). Jiang C, Wang X, Gunawidjaja R, Lin YH, Gupta M, Kaplan DL, Naik RR, Tsukruk VV. Adv. Funct. Mater. 2007; 17:2229–2237.
(53). Vinogradova OI. J. Phys: Condens. Matter. 2004; 16:R1105–R1134.
(54). Heuvingh J, Zappa M, Ferry A. Langmuir. 2005; 21:3165–3171. [PubMed: 15780000]
(55). Gupta MK, SingamanenI S, McConney V, Drummy LF, Naik RR, Tsukruk VV. Adv. Mater. 2010; 22:115–119. [PubMed: 20217709]
(56). Shulha H, Wang CP, Wang DL, Tsukruk VV. Polymer. 2006; 47:5821–5830.
(57). Kozlovskaya V, Sukhishvili SA. Macromolecules. 2006; 39:6191–6199.
(58). Mendelsohn JD, Barrett CJ, Chan VV, Pal AJ, Mayes AM, Rubner MF. Langmuir. 2000; 16:5017–5023.

(59). Sukhorukov GB, Fery A, Brumen M, Möhwald H. Phys. Chem. Chem. Phys. 2004; 6:4078–4098.

(60). Brissova M, Petro M, Lacik I, Powers AC, Wang T. Anal. Biochem. 1996; 242:104–111. [PubMed: 8923972]

(61). Robitaille R, Leblond V, Bourgeois Y, Henley N, Loignon M, Halle JP. J. Biomed. Mater. Res. 2000; 50:420–427. [PubMed: 10737885]

(62). Nuidin N, Canaple L, Bartkowiak V, Desvergne B, Hunkeler D. J. Appl. Polym. Sci. 2000; 75:1165–1175.

(63). Gong D, Yadavalli V, Padavalli M, Paulose M. Biomedical Microdevices. 2003; 51:75–80.

(64). Wilson JT, Cui W, Chaikof EL. NanoLetters. 2008; 8:1940–1948.

(65). Wilson JT, Cui W, Kozlovskaya V, Kharlampieva E, Pan D, Qu Z, Krishnamurthy VR, Mets J, Kumar V, Wen J, Song Y, Tsukruk VV, Chaikof EL. J. Am. Chem. Soc. 2011; 133:7054–7064. [PubMed: 21491937]

(66). Carter JL, Drachuk I, Harbaugh S, Kelley-Loughnane N, Stone M, Tsukruk VV. Macromolecular Bioscince. 2011; 11:1244–1253.

(67). Zhang F, Wu Q, Chen V, Zhang V, Lin XF. J. Colloid Interface Sci. 2008; 317:477–484. [PubMed: 17931643]

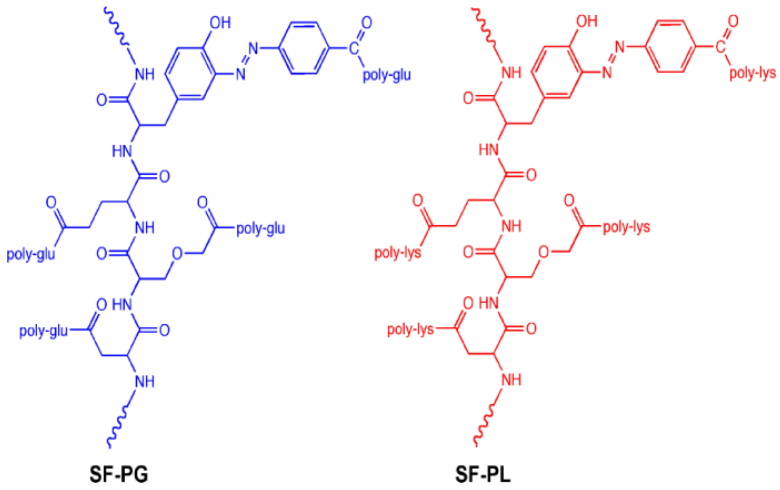

Figure 1.
Chemical structure of silk-poly(amino acid) ionomers: silk-poly(glutamic) acid (SF-PG) and silk-poly(lysine) (SF-PL) exploited in this study.

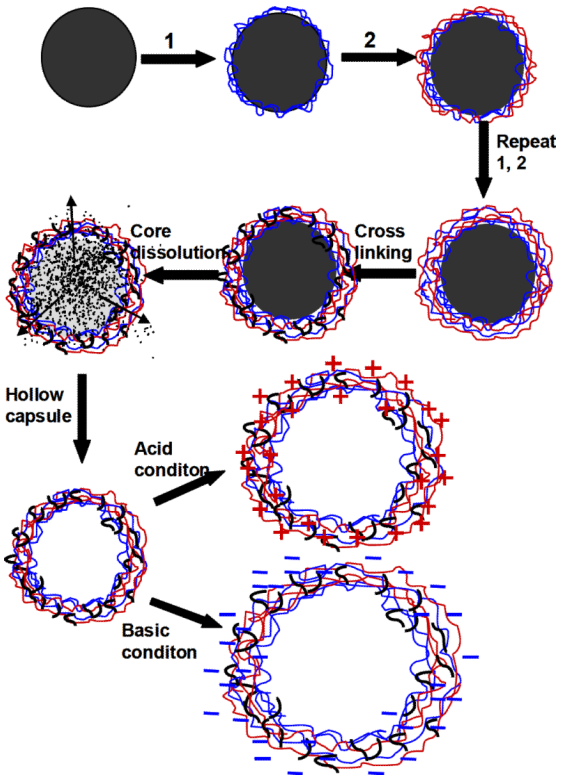

Figure 2.
Schematic illustration of the procedure for preparation of silk ionomer microcapsule.

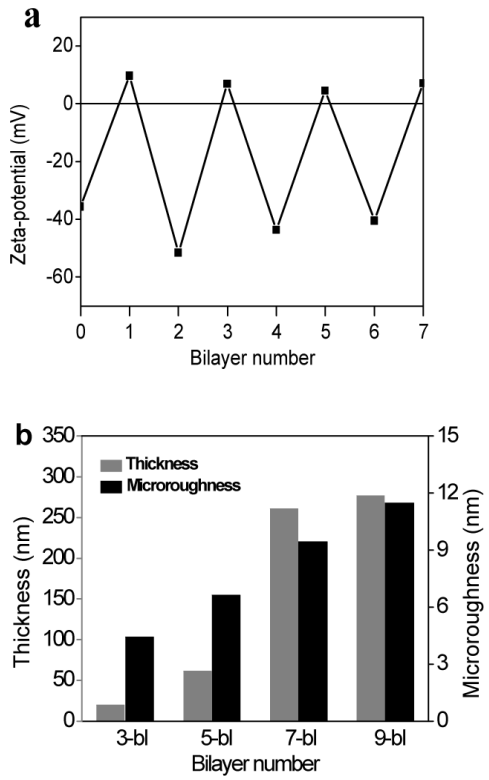

Figure 3.

(a) Variation in the z-potential during the fabrication of PEI-(SF-PG/SF-PL)$_n$ shells on silica sphere; 0 corresponds to the bare silica sphere, 1 corresponds to PEI pre-layer; (b) Shell thickness and microroughness for silk ionomer shells with different bilayer numbers.

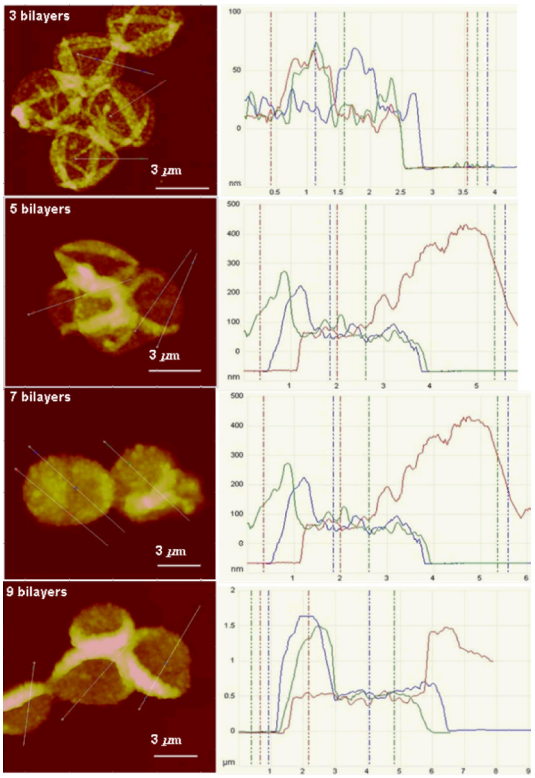

Figure 4.
AFM cross-section analysis of silk ionomer capsules with different bilayers

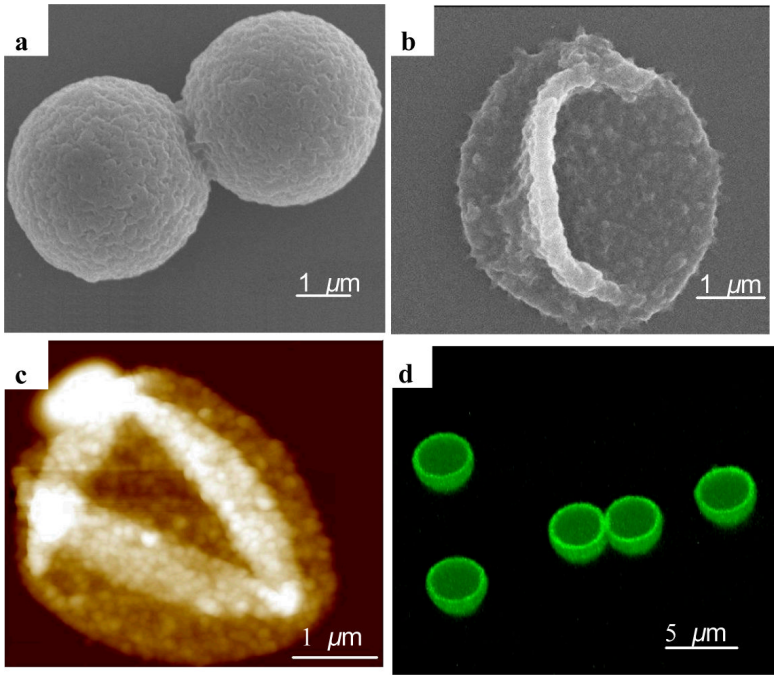

Figure 5.
Morphology of silk ionomer capsules. (a) SEM image of PEI-(SF-PG/SF-PL)$_7$ capsule with silica core; (b) SEM image of PEI-(SF-PG/SF-PL)$_9$ capsule after core dissolution; (c) AFM topography image of dried PEI-(SF-PG/SF-PL)$_5$ capsule (z-scale: 500 nm); (d) 3D confocal image of the PEI-(SF-PG/SF-PL)$_5$ capsule shell labeled with FITC

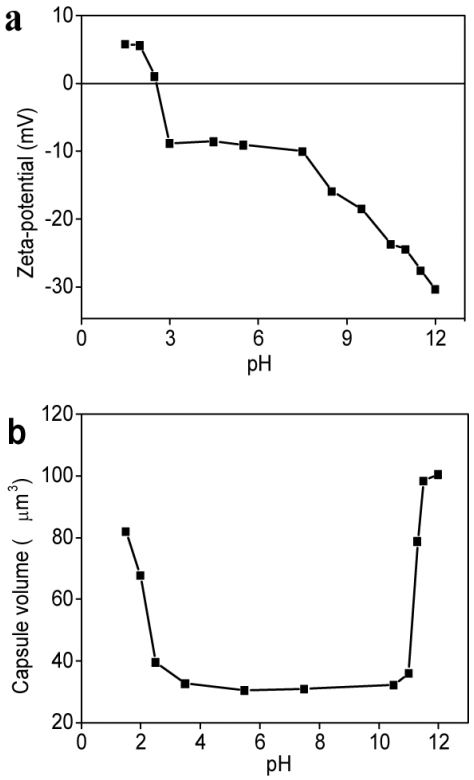

Figure 6.

pH induced responsive properties of silk base capsules. (a) Variation in the z-potential for PEI-(SF-PG/SF-PL)$_3$ hollow capsule as a function of pH; (b) pH-trigged swelling of PEI-(SF-PG/SF-PL)$_9$ hollow capsule in wide pH range from1.5 to 12.0

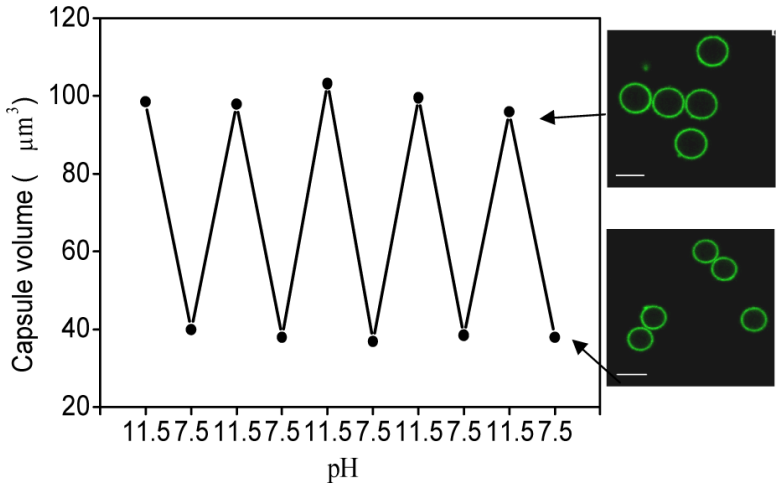

Figure 7.
Reversible volume responsible property of PEI-(SF-PG/SF-PL)$_9$ hollow capsules during alternating pH treatment, arrow indicates the CLSM image of capsules at corresponding pH after five pH cycle treatments. Scale bar is 5 μm.

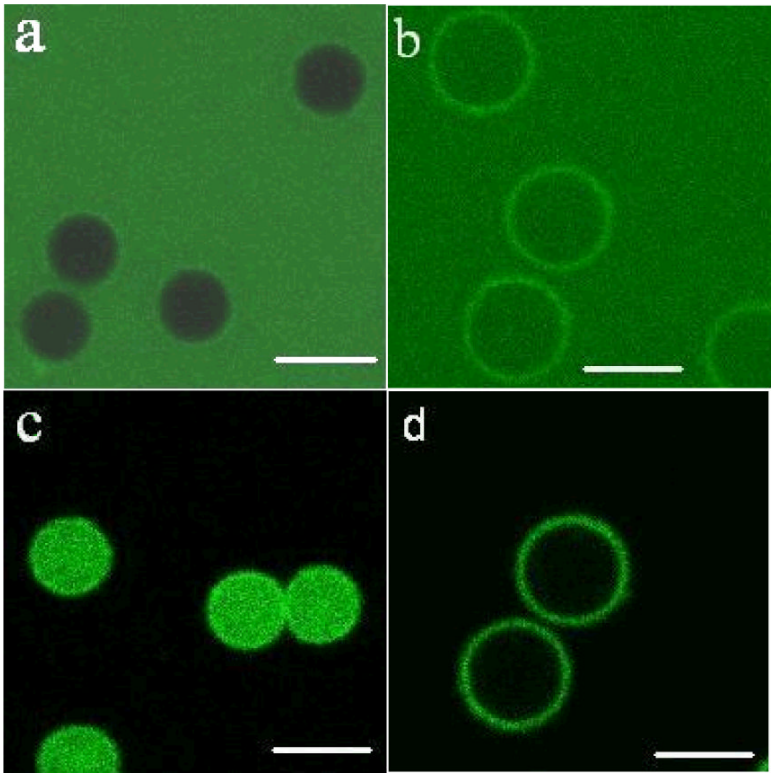

Figure 8.
Confocal microscopy images of encapsulation and release properties of PEI-(SF-PG/SF-PL)$_9$ to 20 kDa FITC-Dextran in phosphate solution with different pH. (a) PEI-(SF-PG/SF-PL)$_9$ capsules exposed to 20 kDa FITC-Dextran solution at pH 5.5. (b) PEI-(SF-PG/SF-PL)$_9$ capsules exposed to 20 kDa FITC-Dextran solution at pH 11.5. (c) Capsules in figure "b" adjusted to pH 7.5. (d) Capsules in figure "c" adjusted to pH 11.5. Scale bar is 5 μm

Table 1

Permeability of PEI-(SF-PG/SF-PL)n capsules with different bilayer numbers to FITC-dextrans solution with varied molecular weight in phosphate solution at pH 5.5

Mw Layer	4 kDa	10 kDa	20 kDa	40 kDa	70 kDa	150kDa	250 Da	500 kDa	2000 kDa
3-bl	+	+	+	+	+	+	+	+	+
5-bl	+	+	+	+	±	−	−	−	−
7-bl	+	−	−	−	−	−	−	−	−
9-bl	+	−	−	−	−	−	−	−	−

Symbols “+”, “−” and “±” indicate permeable, impermeable and partially permeable capsules, respectively.